data

MDPI

Data Descriptor

Non-Destructive Wood Analysis Dataset: Comparing X-Ray and Terahertz Imaging Techniques

Caroline Marc *, Bertrand Marcon, Louis Denaud and Stéphane Girardon

Arts et Metiers Institute of Technology, LaBoMaP, Université Bourgogne Franche-Comté, F-71250 Cluny, France; bertrand.marcon@ensam.eu (B.M.)
* Correspondence: caroline.marc@ensam.eu

Abstract: Wood density measurement plays a crucial role in assessing wood quality and predicting its mechanical performance. This dataset was collected to compare the accuracy and reliability of two non-destructive techniques, X-rays and terahertz waves, for measuring wood density. While X-rays have been commonly used in the industry due to their effectiveness, they pose health risks due to ionizing radiation. Terahertz waves, on the other hand, are non-ionizing and offer high spatial resolution. This article presents a database of wood samples measurements obtained using both techniques, on the same 110 samples with a fine location of the measuring points, on a wide range of wood species (tropical and temperate ones) and densities, from 111 kg·m^{-3} to 1086 kg·m^{-3}. The database includes X-ray and terahertz scans, sample dimensions, moisture content, and color photographs.

Dataset: Dataset is available at https://doi.org/10.57745/RITX8A, accessed on 24 October 2024.

Keywords: wood; terahertz; FMCW radar; X-ray; local density

Citation: Marc, C.; Marcon, B.; Denaud, L.; Girardon, S. Non-Destructive Wood Analysis Dataset: Comparing X-Ray and Terahertz Imaging Techniques. *Data* **2024**, *9*, 130. https://doi.org/10.3390/data9110130

Academic Editor: Giuseppe Ciaburro

Received: 12 September 2024
Revised: 24 October 2024
Accepted: 29 October 2024
Published: 5 November 2024

1. Summary

The mechanical and physical properties of wood, along with its renewable nature, make it a relevant material for designing structural elements in the vehicle and construction industries. However, wood is a natural material that exhibits a high degree of variability. It is a heterogeneous material, with density variations occurring at different scales, including its growth rings, tree, and species levels. Among other parameters, such as moisture content, grain orientation, and wood species, density measurement plays a crucial role in assessing the wood material quality, predicting its mechanical performance [1], and determining its suitability for various applications. This study focusses on measuring wood density using two non-destructive imaging techniques to evaluate the local density: X-rays and terahertz waves.

X-rays are widely employed in materials science to characterize the physical properties of wood. The interactions between X-rays and matter provide valuable information about the structure and composition of samples. When it comes to measuring wood density, X-rays can estimate this property by analyzing the attenuation of X-rays as they pass through the sample. Previous studies have demonstrated the effectiveness of this method in estimating wood density with reasonable accuracy [2–4], making it the most commonly used technique in the industry.

However, despite the excellent resolution and precision offered by X-rays for density measurement in wood, they have a significant drawback that terahertz waves, which will be discussed subsequently, do not possess, i.e., X-rays are ionizing radiation, requiring heavy safety infrastructure to limit health risks. The primary objective of this study is

to compare the accuracy and reliability of both methods to determine the feasibility of replacing X-rays with a non-ionizing technology.

The terahertz domain (THz) corresponds to electromagnetic waves with frequencies ranging from 0.1 to 10 THz, situated between infrared waves and microwaves at the boundary of electronics and optics. Due to the relatively low energy of photons associated with this frequency range (on the order of millielectronvolts, approximately 1000 times smaller than the energy of transitions between electronic levels of atoms), the interactions between terahertz waves and matter are limited to low-energy phenomena. As a result, terahertz radiation is non-ionizing and poses minimal, if any, health risks [5]. Moreover, the properties of terahertz waves enable them to penetrate certain materials that are opaque to visible light [6], offering numerous applications in fields such as security, medicine, pharmacology, materials science, and industrial quality control [7]. THz waves are strongly absorbed by liquid water and water vapor, but their relatively short wavelengths allow for high spatial resolution (from 3 mm to 0.03 mm), making terahertz imaging a powerful and precise technology. However, the study and utilization of terahertz waves only gained prominence in the 1980s, primarily due to the lack of sufficiently efficient sources and detectors. These technical challenges arise from the lack of efficient and compact sources capable of directly emitting radiation in the terahertz frequency range, a region commonly referred to as the 'terahertz gap'. Therefore, either an optical source with its frequency divided or a high-frequency electronic source with its frequency multiplied must be employed. Additionally, the lower energy and longer wavelengths of terahertz photons make their detection fundamentally different from that of radio waves or visible light, requiring specialized techniques such as bolometric or pyroelectric detectors instead of traditional electronic or photonic detectors [6]. Presently, the emergence of new techniques and technologies has contributed to the rapid growth of terahertz research. However, compared to other techniques like X-rays, for instance, terahertz measurement of wood density is less documented in the literature. Several studies have demonstrated a strong relationship between the absorption coefficient of wood at terahertz frequencies and its density using sources such as photoconductive antennas [8] or a Gunn diode [9]. In this study, the measurements performed by a terahertz frequency-modulated continuous-wave (THz FMCW) radar, which is a type of radar system that continuously transmits a periodic signal with varying frequency to detect and measure the velocity and distance of objects and has not been widely explored as a wood density measurement tool before [10], will be analyzed.

The database presented in this article provides the results of measurements obtained using both techniques on samples representing a wide range of wood species and densities, ranging from 111 kg.m^{-3} to 1086 kg.m^{-3}.

2. Data Description

The dataset is available at https://doi.org/10.57745/RITX8A (accessed on 24 October 2024) [11]. The dataset consists of a compressed folder, "THz_XR_RGB_Wood_Dataset.zip", which contains four folders, corresponding to the four types of measurement carried out. The files organization is the following:

- THz_XR_RGB_Wood_Dataset.zip
  - THz
    - Diverse_THz.npy
    - Tropical_THz.npy
  - X_ray
    - Diverse_XR.npy
    - Tropical_XR.npy
  - Specifications
    - Diverse_ specifications.csv
    - Tropical_ specifications.csv

- RGB
  - Diverse
    - FaceNuber_ID.png
    - ...
  - Tropical
    - FaceNuber_ID.png
    - ...

As mentioned later on, the 110 samples studied are divided into two distinct groups: the 'Diverse' group (78 samples) and the 'Tropical' group (32 samples). The THz files, Diverse_THz.npy and Tropical_THz.npy, each contain a Python array of complexes with sizes (78, 140, 73, 512) and (32, 140, 73, 512), respectively. The first axis of the array corresponds to the sample number, with the order indicated in the _dimensions.csv files being alphabetical for the species and after within increasing thickness. The second and third axes of the arrays correspond to the pixels (center of the spot measurement) location in the coordinate system y- and x- axes in millimeters of the samples, as illustrated in Figure 1. Finally, for each sample and position (x, y) on its surface, there is a complex temporal signal obtained using the radar. This signal, sampled at a frequency of 1.8 MHz, can be related to the depth within the sample once transformed into the frequency domain (Equation (1)).

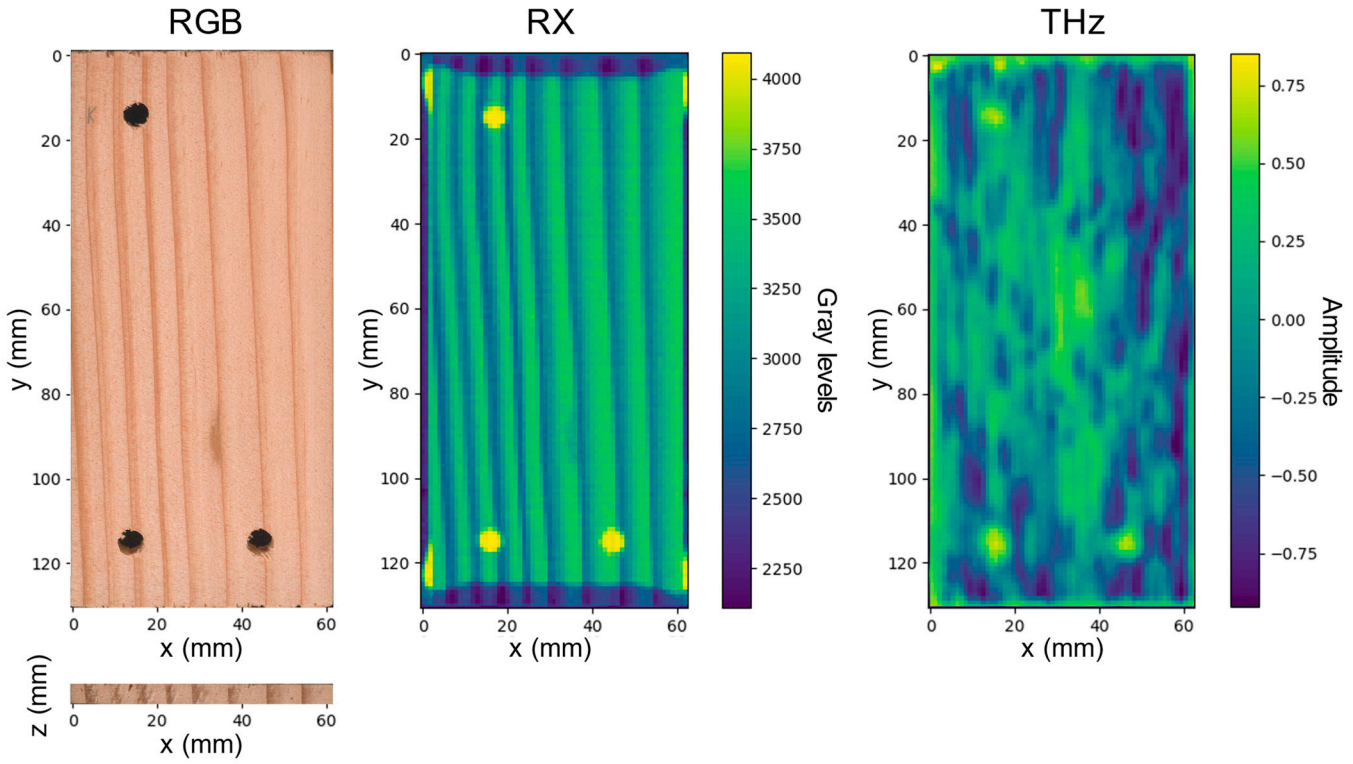

Figure 1. RGB image, X-ray scan, and amplitude map of the first element of the resulted signal from THz scan of a radial Douglas fir sample.

The X-rays files, Diverse_XR.npy and Tropical_XR.npy, also contain Python arrays of grayscale images with sizes (78, 135, 185) and (32, 135, 185), respectively. Here too, the first axis refers to the sample, and the following two axes correspond to the position within the sample.

All sample dimensions and moisture content are included in the Diverse_specifications.csv and Tropical_specifications.csv files, where each row corresponds to a sample. The first column indicates the unique sample identifier, and the second column indicates the species. The identifiers consist of three letters and are constructed differently for the two groups.

For the Tropical group, it is simply the first three letters of the sample's species (e.g., "Oko" for Okoume). For the Diverse group, a letter indicating the sample thickness is combined with the first two letters of the species. The letters indicating thickness range from A to L, with A to D representing samples of ~1 mm, E to H representing samples of ~3 mm, and I to L representing samples of ~5 mm. For the Douglas fir samples, the tangential and radial cuts are differentiated by having "DT" and "DR" as the last two letters of their identifiers, respectively. For example, a 5 mm thick Douglas radial sample is identified as "JDR", and a 1 mm thick oak sample is named "COa".

Regarding the color images, each photo is named using the face number and sample ID.

3. Methods

3.1. Samples

A total of 110 samples were scanned, measuring 130 mm × 60 mm with variable thicknesses. These samples are divided into two groups, hereinafter referred to as the Diverse group and the Tropical group.

The Tropical group consists of 32 samples obtained from a xylotheque (library of wooden samples well identified and stored) of tropical woods from Africa and Asia, with a thickness of 9 ± 1 mm. The 32 species are as follows: Aiele (*Canarium schweinfurthii*), African mahogany (*Khaya anthotheca*), Ako (*Antiaris toxicaria*), Avodire (*Turraeanthus Africanus*), Azobe (*Lophira alata*), Bete (*Mansonia altissima*), Bosse (*Guarea cedrata*), Bubinga (*Guibourtia demeusei*), Dau (*Xylopia* spp.), Dibetou (*Lovoa trichilioides*), Doussie (*Afzelia Africana*), Framire (*Terminalia ivorensis*), Ilomba (*Pycnanthus angolensis*), Iroko (*Milicia excelsa*), Kossipo (*Entandrophragma candollei*), Kotibe (*Nesogordonia papaverifera*), Limba (*Terminalia superba*), Makore (*Tieghemella africana*), Niangon (*Heritiera utilis*), Niove (*Staudtia kamerunensis*), Okoume (*Aucoumea klaineana*), Olon (*Fagara heitzii*), Ozigo (*Dacryodes buettneri*), Rosewood (*Dalbergia* spp.), Cam Laï Rosewood (*Dalbergia* spp.), Rosewood Trac (*Dalbergia cochinchinensis*), Samba (*Triplochiton scleroxylon*), Sapelli (*Entandrophragma cylindricum*), Sipo (*Entandrophragma utile*), Teak (*Tectona grandis*), Tiama (*Entandrophragma angolense*), Zingana (*Microberlinia bisulcata*). The samples were obtained from cuts that varies between radial and tangential (cf. Figure 2a).

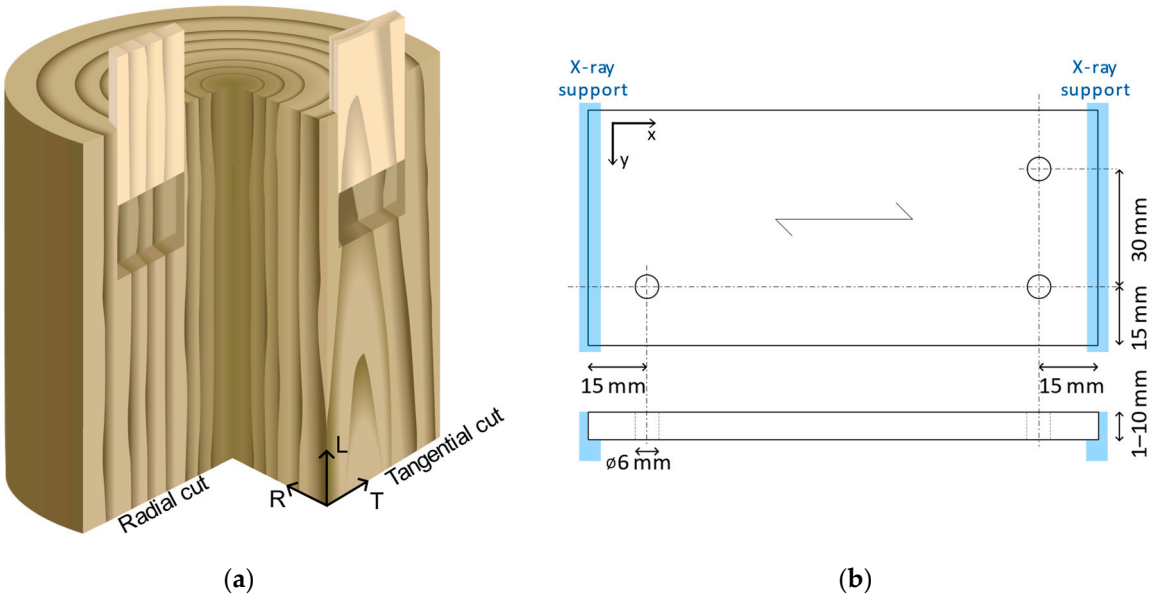

(**a**) (**b**)

Figure 2. (**a**) Direction and cut of wood, with a radial sample and a tangential sample, (**b**) sample dimensions; the three going through holes are performed to avoid any inaccurate localization between X-rays and THz scans and to help overlap both scan data sets.

The Diverse group consists of 78 samples manufactured specifically for this study, using 6 different wood species: balsa (*Ochroma pyramidale*), beech (*Fagus sylvatica*), red cedar (*Thuja plicata*), Douglas fir (*Pseudotsuga menziesii*), poplar (*Populus Tremula*), and oak (*Quercus Robur*). The samples were also obtained from cuts that varies between radial and tangential, except for the Douglas fir samples, which were divided into two *subcategories*: radial cut and tangential cut. There are three different thicknesses: 1 mm, 3 mm, and 5 mm. Each combination of species and thickness (and cuts in the case of Douglas) is replicated 4 times, except for the 1 mm thick samples of Poplar, radial Douglas fir, and tangential Douglas fir, which are replicated 2 times each.

The overall density of the samples ranges from 111 kg·m^{-3} to 1086 kg·m^{-3}, as shown in Figure 3.

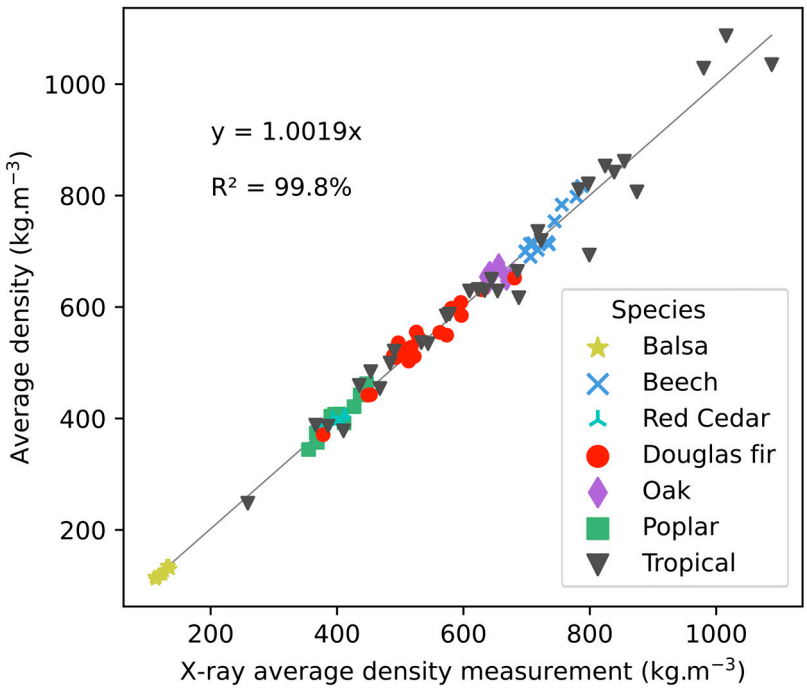

Figure 3. Average measured density versus average X-ray density.

To facilitate alignment *between* different measurement methods, the samples were drilled with through holes measuring 6 mm in diameter, located at 3 of their corners, as illustrated in the Figure 2b.

3.2. Measurement

3.2.1. X-Ray Imaging

In order to determine their local density, the samples were passed through an industrial optical scanner equipped, among other measurements, with an X-ray by transmission imaging system. The obtained data consist of two-dimensional map of 12-bit (from 0 to 4095 gray levels). The gray levels are proportional to the transmitted wave intensity, which are, therefore, related to the density and thickness of the sample considering the Beer–Lambert law [12]. The power of the X-ray source was previously adjusted (35 kV, 35 mA) so that the images do not exhibit saturation either in the dark or in the bright areas. The spatial resolution of the images is 1 mm.px^{-1} in the grain direction (length of the samples) and 0.34 mm.px^{-1} in the other direction (width of the samples).

Since the scanner is designed for measuring boards, the samples had to be placed on a support during the measurements. The transmitted intensity is, thus, distorted where the samples are held on the support, specifically on a strip of approximately 2 mm at each end (Figures 1 and 2b).

Figure 3 illustrates the accuracy of X-ray density measurement, showing an R^2 coefficient of determination of 99.8% between the actual average density per sample and the average density obtained by X-ray.

3.2.2. THz Frequency-Modulated Continuous-Wave (FMCW) Radar Imaging

Measurements at terahertz frequencies were conducted using an FMCW radar (Terascan 100 equipped with a 50 mm focal lens, Lytid, Figure 4).

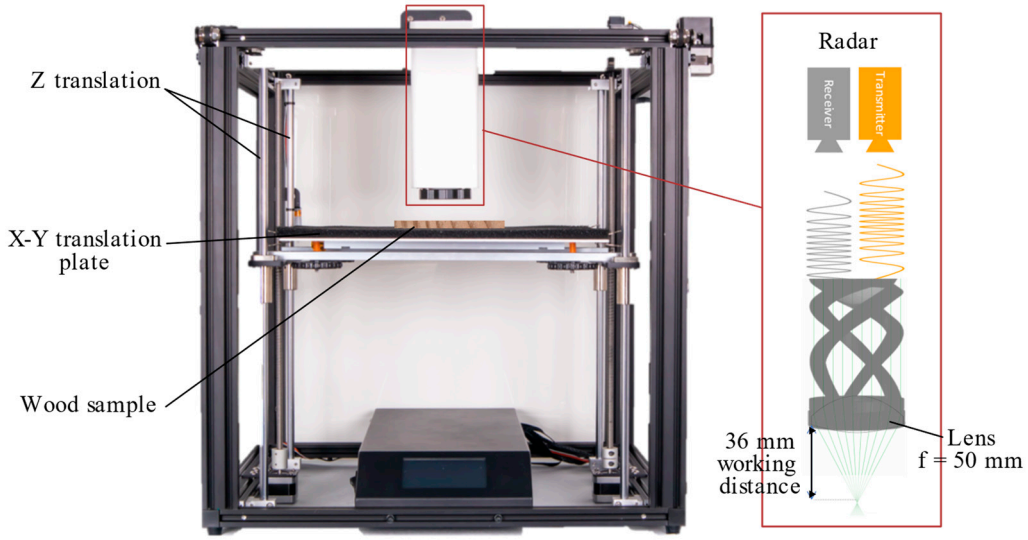

Figure 4. FMCW radar Terascan 100, Lytid.

The operating principle of the FMCW radar [13], illustrated in Figure 5, is as follows: a signal is generated by a voltage-controlled oscillator with a gradually changing frequency (ranging from 110 GHz to 130 GHz) through triangular modulation. This signal is then multiplied in frequency and then transmitted to the target via a transmitting antenna. When the signal encounters an interface between two materials with different optical indices, part of it is reflected back towards the radar system.

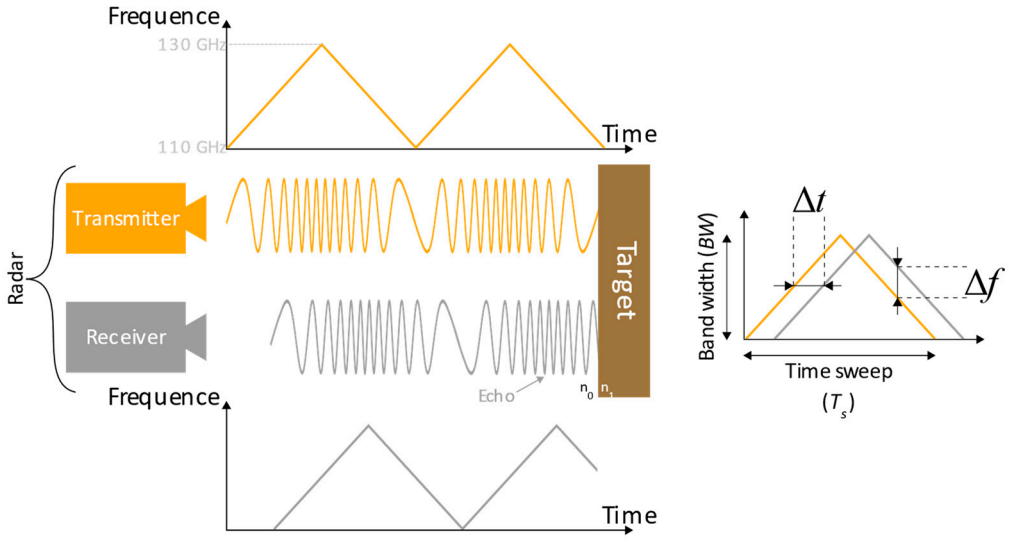

Figure 5. Operating principle of a FMCW radar.

The proportion of the reflected signal depends, among other factors such as material heterogeneity, on the optical index of the material. The optical index refers to the complex

refractive index, which includes both the real part (refractive index) and the imaginary part (absorption coefficient). The reflected signal is then received and mixed with a local reference signal to produce the beating signal. The frequency of this beating signal (Δf in Figure 4) is directly related to the distance between the radar and the target. If multiple targets or interfaces are encountered along the signal's path (e.g., irregularities in the sample or the backside of the sample), the beat signal can be decomposed into multiple sinusoidal components, each corresponding to a different interface and, thus, a different interface radar distance. By analyzing the beating signal, information about the materials the wave interacted with can be obtained, as well as determine the position of these interfaces relative to the radar.

Equation (1) gives the relation between the distance to the target (z) and the beating signal frequency (Δf):

$$z = \frac{c \times \Delta t}{2n} = \frac{c \times \Delta f \times T_s}{2n \times BW} \quad (1)$$

with c is the speed of light ($\mathrm{m \cdot s^{-1}}$), Δt is the time delay between emitted and received signal (s), n is the optical index (-) of the propagation medium under those specific THz frequency range, T_s is the sweep time (283.889 µs), and BW is the sweep bandwidth (19.505 GHz). The sampling frequency is 1.8 MHz.

Prior to measuring the samples, the radar is calibrated by first performing a background measurement, followed by a reference measurement using a metallic mirror positioned at the waist focal point of the optical setup. This enables certain optical-related noise, such as interference from optical elements like lenses, to be filtered out, and the plane of the mirror is set as the reference plane, i.e., the point of zero beating frequency. To perform the measurements, the samples are positioned on the mirror, which has been moved away from the radar by a distance equal to the thickness of the sample being measured, so that the focal point is at the level of the first face of the sample encountered by the waves. The measurement grid resolution is 1 mm per pixel in both directions, namely, x and y (in Figure 2b). However, this is distinct from the spatial resolution of the system, which is primarily determined by the wavelength corresponding to the frequency range of 110 to 130 GHz (corresponding to wave lengths of 2.7 and 2.3 mm) in the FMCW setup, resulting in a lateral spatial resolution of approximately 1.8 mm (from Lytid technical data with the 50 mm focal lens).

3.2.3. Dimensions

The dimensions of the samples (length, width, thickness) were measured using a digital caliper (resolution 0.01 mm). Their mass was measured using a Kern balance (resolution 0.01 g) shortly before the THz and X-ray measurements. The overall density was calculated based on these data, while considering the volume occupied by the holes.

3.2.4. Moisture Content

The samples were not humidity-stabilized in a climatic chamber prior to measurement, but simply exposed to ambient air, assuming that their humidity was stabilized to the ambient conditions in the laboratory as the duration of THz measurement (approximately 40 min per specimen) cannot ensure the non-variation of moisture content (MC) in the specimens. After the scans, the samples were placed in a climatic chamber set at 30 °C and 50% relative humidity, and their masses ($m_{9\%}$) were recorded at 9% of equilibrium MC ($MC_{9\%}$), which was close to the supposed equilibrium MC in ambient conditions. Based on these measurements and knowing the mass of the samples at the time of the X-ray and THz scans (m_t), their overall moisture content at the time of the measurements (H_t) could be obtained using Equation (2) using the definition of MC [14].

$$MC_t = MC_{9\%} + \frac{m_{9\%} - m_t}{m_{9\%}}(1 + MC_{9\%}) \quad (2)$$

3.2.5. RGB Images

The six faces of each sample were scanned using a flatbed scanner to obtain a high-resolution color image (0.042 mm·px^{-1}) of the external surface of all samples. As shown in Figure 6, faces 1 and 2 correspond to the two largest faces of the samples, faces 3 and 4 represent the cross-sections of the samples mainly in the longitudinal direction (length of the samples), and, finally, faces 5 and 6 represent the cross-sections of the samples in the RT plane (width of the samples).

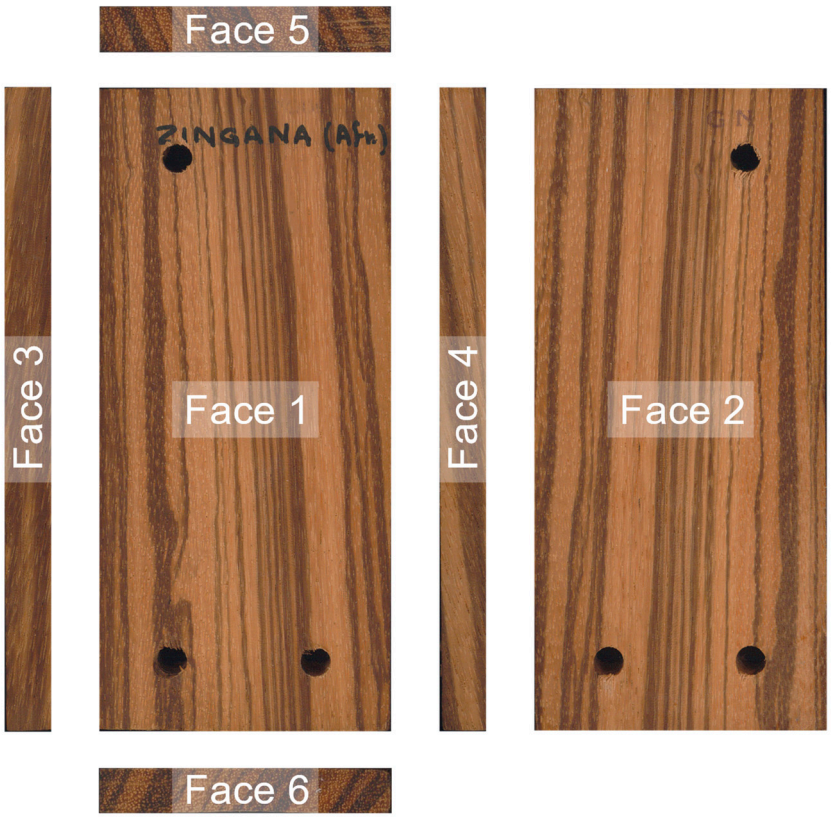

Figure 6. Faces of a Tropical sample (Zingana).

Author Contributions: C.M.: methodology, writing—original draft, data curation; B.M.: supervision, writing—review and editing; L.D.: supervision, writing—review and editing; S.G.: supervision, writing—review and editing. All authors have read and agreed to the published version of the manuscript.

Funding: This work is funded by the ANR-21-CE43-0008-02 project.

Institutional Review Board Statement: Not applicable.

Informed Consent Statement: Not applicable.

Data Availability Statement: The original data presented in the study are openly available in Recherche Data Gouv at https://doi.org/10.57745/RITX8A, accessed on 24 October 2024.

Acknowledgments: The authors thank Michel Badin for providing the xylotheque used in this study, and the technical platform Xylomat of the scientific network Xylomat financed by the ANR-10-EQPX-16 XYLOFOREST, which was largely used to carry out this work.

Conflicts of Interest: The authors declare that they have no known competing financial interests or personal relationships that could have appeared to influence the work reported in this paper.

References

1. Zobel, B.J.; Van Buijtenen, J.P. *Wood Variation: Its Causes and Control*; Springer Science & Business Media: Berlin/Heidelberg, Germany, 2012.
2. Bergsten, U.; Lindeberg, J.; Rindby, A.; Evans, R. Batch measurements of wood density on intact or prepared drill cores using X-ray microdensitometry. *Wood Sci. Technol.* **2001**, *35*, 435–452. [CrossRef]
3. Decoux, V.; Varcin, E.; Leban, J.M. Relationships between the intra-ring wood density assessed by X-ray densitometry and optical anatomical measurements in conifers. Consequences for the cell wall apparent density determination. *Ann. For. Sci.* **2004**, *61*, 251–262. [CrossRef]
4. Freyburger, C.; Longuetaud, F.; Mothe, F.; Constant, T.; Leban, J.M. Measuring wood density by means of X-ray computer tomography. *Ann. For. Sci.* **2009**, *66*, 804. [CrossRef]
5. Vander Vorst, A.; Rosen, A.; Kotsuka, Y. *RF/Microwave Interaction with Biological Tissues*; John Wiley Sons: Hoboken, NJ, USA, 2006.
6. Pawar, A.Y.; Sonawane, D.D.; Erande, K.B.; Derle, D.V. Terahertz technology and its applications. *Drug Invent. Today* **2013**, *5*, 157–163. [CrossRef]
7. Dragoman, D.; Dragoman, M. Terahertz fields and applications. *Prog. Quantum Electron.* **2004**, *28*, 1–66. [CrossRef]
8. Koch, M.; Hunsche, S.; Schuacher, P.; Nuss, M.C.; Feldmann, J.; Fromm, J. THz-imaging: A new method for density mapping of wood. *Wood Sci. Technol.* **1998**, *7*, 421–427. [CrossRef]
9. Chulkov, A.O.; Pradere, C.; Puiggali, J.R.; Batsale, J.C.; Vavilov, V.P. Estimating the humidity of wood by terahertz infrared thermography. *Russ. J. Nondestruct. Test.* **2016**, *52*, 753–757. [CrossRef]
10. Marc, C.; Marcon, B.; Denaud, L.; Girardon, S.; Butaud, J.-C. Preliminary performance evaluations of non-ionizing Terahertz wood densitometry. In Proceedings of the 20th International Conference on Experimental Mechanics (ICEM20): Experimental Mechanics in Engineering and Biomechanics, Porto, Portugal, 2–7 July 2023.
11. Marc, C.; Marcon, B.; Denaud, L.; Girardon, S. *Multispectral Wood Analysis Dataset: X-Ray, Terahertz, and Visible Light Imaging, V1 ed.*; Recherche Data Gouv; Arts et Métiers Sciences & Technologies: Paris, France, 2024. [CrossRef]
12. Kim, K.M.; Lee, S.J.; Lee, J.J. Development of portable X-Ray CT system 1-evaluation of wood density using X-Ray radiography. *J. Korean Wood Sci. Technol.* **2006**, *34*, 15–22.
13. Jankiraman, M. *FMCW Radar Design*; Artech House: Houston, TX, USA, 2018; 430p.
14. Simpson, W.T. *Specific Gravity, Moisture Content, and Density Relationship for Wood*; General Technical Report FPL-GTR-76; U.S. Department of Agriculture, Forest Service, Forest Products Laboratory: Madison, WI, USA, 1993; pp. 1–13. Available online: https://www.fpl.fs.usda.gov/documnts/fplgtr/fplgtr76.pdf (accessed on 24 October 2024).